Simulation of the space-time evolution of nonequilibrium phonons in GaAs by the Monte Carlo method

B. A. Danil'chenko, D. V. Kazakovtsev, and I. A. Obukhov

Institute of Solid State Physics, Russian Academy of Sciences; 142434 Cherngolovko, Moscow Region, Russia; Institute of Physics, Ukrainian Academy of Sciences, 252650 Kiev, Ukraine
(Submitted 6 March 1993)
Zh. Eksp. Teor. Fiz. **106**, 1439–1452 (November 1994)

In this paper we calculate the shapes of time-of-flight spectra of nonequilibrium acoustic phonons recorded by a wideband detector for initially monochromatic phonons generated with various frequencies and polarizations in a crystal of GaAs. The shapes are calculated within a quasi-isotropic model, taking into account elastic scattering of the phonons by isotopes and three-phonon inelastic spontaneous decay processes. We show that changes in the intensity of the latter fundamentally change the shape of the time-of-flight spectra. Our results enable us to explain the origin of a number of peculiarities in the shape of nonequilibrium phonon pulses observed experimentally when a semiconductor surface is optically excited. © *1994 American Institute of Physics.*

1. INTRODUCTION. FORMULATION OF THE PROBLEM

For many experiments in which phonon pulses are created in semiconductors and insulators at low temperatures, the source of nonequilibrium acoustic phonons is the nonradiative relaxation of optical excitations of the electronic system.[1,2] In the course of this excitation, nonequilibrium acoustic phonons are created over a wide range of frequencies with a maximum at a characteristic frequency of the same order as the Debye frequency.[1,3–5] Even in the most perfect crystals, these high-frequency phonons have a short mean free path, due to scattering both by isotopes and other point defects and to inelastic anharmonic processes. Nevertheless, phonon pulses are usually recorded at macroscopic distances from the source; hence, the generation of these pulses from an initial excitation of high-frequency phonons must involve processes whereby a phonon excitation that is far from equilibrium propagates in the crystal, accompanied by relaxation of its energy. The term "far from equilibrium" is defined by the presence in the original spectrum of occupation numbers that are larger than the equilibrium value $n_T(\omega)$ corresponding to the temperature T of the surrounding heat bath for phonons with frequencies on the order of the Debye frequency. At the same time, the occupation numbers of nonequilibrium phonons for all frequencies $\omega \gg \omega_T$ can remain small in the course of their subsequent evolution, i.e.,

$$n \ll 1. \tag{1}$$

As long as this condition is satisfied, the energy relaxation of nonequilibrium phonons in the crystal is determined only by their spontaneous decay processes.

Despite this simplification, a systematic analytic description of the kinetics of nonequilibrium acoustic phonons under these conditions is very difficult. The distribution functions $N_{L,T}(t, \mathbf{r}, \mathbf{k})$ for the longitudinal and transverse phonon branches in the solid satisfy the kinetic equations

$$\frac{\partial N_{L,T}}{\partial t} + \mathbf{w}_{L,T} \frac{\partial N_{L,T}}{\partial \mathbf{r}} = -\frac{N_{L,T} - \langle N \rangle_{\Omega}}{\tau_i(\omega)} + \hat{S}_{L,T} N_{L,T}. \tag{2}$$

Here $\mathbf{w}_{L,T}(\mathbf{k})$ is the group velocity of a phonon belonging to the corresponding branch with quasimomentum $\mathbf{k}$, $\tau_i(\omega)$ is the elastic scattering time for a phonon with frequency ω due to isotopes and other impurities, and $\langle N \rangle_{\Omega}$ is the distribution function for phonons of frequency ω averaged over polarization and the direction Ω of the wave vector $\mathbf{k}$. The operators $\hat{S}_{L,T}$ describe three-phonon anharmonic processes, and have a rather complicated form.[6] However, it is important that these operators, and both of Eqs. (2), can be linearized with respect to N when condition (1) is satisfied.

The most successful attempts at an analytic solution to Eq. (2) under conditions similar to real optical excitation of nonequilibrium phonons were made by Kazakovtsev and Levinson.[7,8] In these papers, the authors placed two more limitations on the region of applicability of the solutions they obtain, in addition to the linearization of the kinetic equations mentioned above, which is a consequence of condition (1). First of all, they assumed that scattering by impurities and isotopes is much stronger than inelastic scattering at all frequencies. Secondly, they investigated the characteristic distances over which these distribution functions vary, and found them to be much larger than the mean free path of the phonons with respect to inelastic processes. This allowed them to reduce the left side of (2), along with the collision integral that describes elastic scattering, to a diffusion equation, with the inelastic collision operators $S_{L,T}$ treated as a small perturbation. However, even with these assumptions their solutions can describe only the primary group of phonons arriving at the detector, and cannot specify the shape of the nonequilibrium phonon pulse in detail.

In practice it is not possible to obtain an analytic solution that describes the space-time evolution of these phonons when the characteristic times for their inelastic scattering and decay are comparable in order of magnitude, and of the same order of magnitude as the time for the phonons to propagate to the detector. Nevertheless, it is just this situation that is realized in many of the experiments involving the detection of phonon pulses generated by optical excitation of an electronic system in a crystal. Finally, the simplified models of

 1063-7761/94/110777-08$10.00

Kazakovtsev and Levinson[7,8] that admit of an analytic solution cannot be used to explain certain features in the shape of the recorded phonon pulses. In particular, the origin of certain commonly observed strong phonon peaks, which judging from their time of arrival are purely ballistic, is not completely clear. At present, the interpretation of the "slow" peak in the recorded shape of the pulse observed by Ulbrich *et al.*[9,10] and Danilchenko *et al.*[2] remains uncertain.

In light of all this, the most promising approach to a quantitative treatment of the experimental results is based on direct computer simulation of the trajectory of each phonon that contributes to the recorded pulse using the Monte Carlo method. Naturally, the quantitative computations must be carried out for a specific crystal in this case. We chose gallium arsenide as our simulation crystal. Our choice is primarily motivated by the widespread use of GaAs-based electronic devices at cryogenic temperatures. When the geometric dimensions are reduced and the operating temperatures are lowered to that of liquid helium, the character of heat transfer in such structures changes qualitatively as they enter the ballistic regime. The GaAs crystal has been rather well studied by traditional methods of ultra- and hypersonic acoustics.[11] Furthermore, it is likely that of all the studies made of the transport of nonequilibrium phonons, those carried out in GaAs have produced the most inconsistent results,[1,9,12–14] and thus have generated the most controversy. Theoretical estimates[6] of the decay times of acoustic phonons in GaAs suggest that it exhibits the closest match between the time for inelastic anharmonic scattering $\tau(\omega)$ and the time for isotopic elastic scattering $\tau_i(\omega)$. This fact allows us to track how the transport regime for nonequilibrium phonons changes as a function of excitation conditions. Incidentally, this match between the acoustic parameters of GaAs may in fact be the reason for the contradictory interpretations of experimental results obtained at various laboratories. It is these facts that explain the great interest in mathematically simulating the kinetics of nonequilibrium phonons in GaAs, especially for values of the parameters for which analytic results are unavailable. In this paper we describe our successful solution to this problem for the simplest case $n \ll 1$, taking into account the elastic scattering of phonons and their decay. In essence, we have solved Eq. (2) numerically for a crystal of GaAs with the simplification (1), but without the limitations imposed in Refs. 7, 8.

Our approach to this problem is similar to that used by Lax *et al.*[12–14] and Wolfe *et al.* However, the goal of those papers was to treat only the "slow peak" observed experimentally by Ulbrich *et al.*[10] The authors of that paper associated this peak with propagation of *TA* phonons at 1.5 THz, their highest frequency, over distances of order one centimeter, and never addressed the overall problem of computing the shape of the time-of-flight spectra for the nonequilibrium phonons generated by the optical excitation. The more accurate decay times in GaAs computed later by Tamura[6] were not known to Lax *et al.*[12] and Wolfe *et al.*[13] Lax *et al.* used those more accurate decay times in Ref. 14; however, in that paper only two time-of-flight spectra were presented for the special case of initially *TA* phonons with a single starting frequency $\nu_0 = 1.5$ THz. Neither of those curves contained the ballistic peaks that are usually present in the experimental curves, even when the isotopic scattering was attenuated by a factor of 10, a step that is hard to justify physically; it will be clear why this is so in what follows. In particular, the paper by Maris[15] shows that interest in simulating the shape of nonequilibrium phonon pulses by Monte Carlo methods has not abated. Here, however, our task will be not so much to solve the problem of simulating the results observed in experiment as to explain the limits of applicability of the theoretical considerations in Refs. 7, 8.

Thus, the problem of calculating the shape of nonequilibrium phonon pulses by the Monte Carlo method is one of no small interest, now that it is possible to include the results obtained by Tamura[6] with a minimum of simplifying assumptions.

2. DESCRIPTION OF THE PHYSICAL PRINCIPLES OF THE MODEL

The experimentally measured parameter that characterizes the kinetics of nonequilibrium phonons in semiconductors is the time-of-flight spectrum. Therefore, the primary goal of our numerical experiment will be to calculate these spectra. Instead of doing our simulations in the geometry used previously by Lax *et al.*,[12] i.e., a plane-parallel film, we investigated the motion of phonons outward from the center of a sphere of radius R. By choosing this model geometry we greatly reduce the number of calculations required while retaining the generality of the results within the framework of an isotropic model phonon spectrum.

In our model, acoustic phonons propagate in a quasi-isotropic elastic medium that most closely matches a GaAs crystal while participating in elastic scattering and spontaneous decay.[6] In this approximation, the average velocity of the *LA* branch is $v_L = 5.13 \cdot 10^5$ cm/s, that of the two degenerate *TA* branches is $v_L = 3.02 \cdot 10^5$ cm/s, and the isotopic scattering time is

$$\tau_i = 1.35 \cdot 10^{4I} \nu^{-4} \text{s}. \tag{3}$$

The lifetime of a *LA* phonon against spontaneous decay due to three-phonon anharmonic processes is taken to be $\tau_0(\nu) = 0.74 \cdot 10^{54} \nu^{-5}$ s, i.e., one of the two values computed by Tamura[6] using the two different sets of experimental parameters for a GaAs crystal. We took the relative probability for the two possible channels by which *LA* phonons can decay from Tamura's paper: the probability α of the channel $LA \rightarrow TA + TA$ is set equal to 0.75, whereas the probability for the channel $LA \rightarrow LA + TA$ is accordingly $1 - \alpha = 0.25$. The *TA* phonons do not decay; however, in elastic scattering the mode conversion $TA(\nu) \rightarrow LA(\nu)$ can occur with a probability proportional to the density of final phonon states. Using the parameters of this model, we find that the probability for conversion of *TA* phonons to the *LA* mode after elastic scattering equals 0.1, while the probability of remaining in the *TA* mode is 0.9. The same ratios for the probabilities are also preserved in scattering of *LA* phonons.

There is an important difference between our model and previous models: we have taken into account the fact that a decay event does not necessarily result in daughter phonons with frequencies that are strictly half that of their parent. The

ratio of the frequencies of the phonons created by the decay can be arbitrary; however, they must be within limits set by the laws of conservation of energy and momentum for acoustic phonons in an elementary decay event. The decay probability distribution that we used, which is a function of the ratio of the frequencies of the final phonons, was analogous to that used by Kazakovtsev *et al.*,[16] with the difference that those authors used parameters for a certain generalized crystal, whereas here the form of the distribution is specific to a GaAs crystal.

Although a detailed description of the computational algorithm our program uses would be of interest in its own right, such a description would greatly complicate the exposition of our material, to the detriment of the physical meaning of the simulation results. Therefore, we give only a brief description here of the fundamental principles that underlie our program.

For each run, we modeled the motion of an individual phonon with initial frequency ν_0 belonging to the *LA* or *TA* modes, which starts from the center of the sphere $R=0$ at time $t=0$. Since the number of phonons is not conserved during a decay, one of the instantaneous parameters is the energy $h\nu$ of that phonon whose motion is being followed at a given time. After a cascade of scatterings with possible branchings during the decays, the total energy $\Sigma_\nu \Delta N h\nu$ of phonons that intersect the surface of the sphere of radius $R=1$ within the time interval from t to $t+\Delta t$, summed over all frequencies, is recorded. After all the phonons created in the decay process have reached the surface of the sphere, we obtain a single histogram for the phonon energy flux. Summing a large number of these histograms then gives the result of the numerical experiment. Actually, the derivative

$$A(t)=\Sigma_\nu \frac{\Delta N h\nu}{\Delta t}$$

describes the phonon energy flux through the surface of the sphere at time t. If the value of $A(t)$ is normalized to the initial energy of the starting phonons $N_0 h\nu_0$, where N_0 is the number of original phonons, then the ratio $\gamma(t)=A(t)/N_0 h\nu_0$ is a measure of the temporal flux density of phonon energy through the surface $R=1$ cm at time t. It is clear that the integral over such a flux density should equal unity,

$$\int_0^\infty \frac{A(t)}{N_0 h\nu_0} dt = 1.$$

This invariant is used as a way of monitoring the accuracy of the computational program in the course of its operation. By defining the quantity $\gamma(t)$ in this way, we can obtain simulation results in units that do not depend on the number of initial startup phonons, although, of course, the accuracy of the resulting function increases as N_0 increases. Usually the number N_0 ranges from 10^4–10^5, and is determined by the precision required to construct the quantity $\gamma(t)$, i.e., sufficient for a quantitative comparison with the experimental time-of-flight spectra.

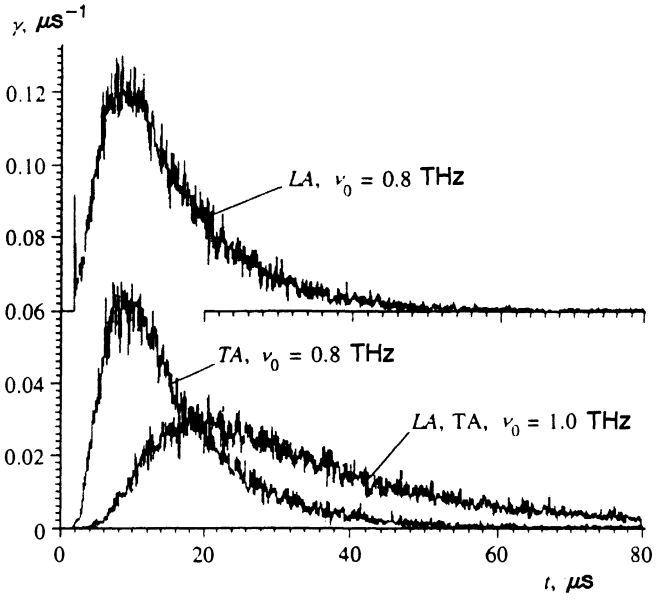

FIG. 1. Computed shapes of time-of-flight spectra for nonequilibrium phonons with initial frequencies ν_0=0.8 and 1.0 THz when only elastic scattering by isotopes is taken into account.

3. MODELING WITH PURE PHONON DIFFUSION

In Fig. 1 we show the results of modeling the phonon flux for initial phonon frequencies ν_0=0.8 and 1.0 THz, taking into account only phonon elastic scattering. It is clear that the character of the propagation is essentially independent of the polarization of the original phonon. This should come as no surprise, since elastic scattering with mode conversion effectively mixes phonons of different polarizations at distances large compared to the phonon mean free path when the propagation regime is close to diffusive. The mean free paths of phonons with ν_0=0.8 THz equal 0.17 and 0.1 cm for the *LA* and *TA* modes, respectively, while at frequencies ν_0=1 THz they are 0.07 and 0.04 cm; thus, all these mean free paths are much smaller than the radius of the sphere $R=1$ cm. In accordance with these estimates, within the limits of noise the curves for initially *LA* and *TA* phonons with ν_0=1 THz coincide completely. However, for phonons belonging to the *LA* mode there exists a finite probability of order $\exp(-1/0.17)=3\cdot10^{-3}$ for ballistic drift over this distance. For a phonon belonging to the *TA* mode this probability is roughly two orders of magnitude smaller, and equals $5\cdot10^{-5}$. This situation is reflected in the results of Fig. 1 by the presence of a sharp ballistic peak with just this probability $3\cdot10^{-3}$ against a background of a broad diffuse pulse for the case where the starting phonon is *LA*.

We can compare the results of our simulations with the analytic expression for the diffusion current, which contains the elastic scattering time $\tau_i(\omega)$ given by (3) and a diffusion coefficient averaged over the branches:

$$D(\omega)=\frac{1}{3}\tau_i(\omega)\frac{v_L+2v_T}{v_L^{-3}+2v_T^{-3}}.$$

For this case we write the diffusion equation in its usual form

$$\frac{\partial N(\omega)}{\partial t}+D(\omega)\Delta N(\omega). \tag{4}$$

Since the phonons that reach the boundary $R=1$ cm are immediately absorbed by it and drop out of the calculation, our formulation of the numerical experiment corresponds to a Green's function for this equation in a sphere of radius $R=1$ cm with the boundary condition

$$N(r)|_R=0. \tag{5}$$

Let us make use of the solution to Eq. (4) in a sphere of finite radius [see Ref. 17, Ch. 9, Sec. 3, Eq. (3.3)]. The boundary condition (5) corresponds to $\varphi(t)=0$. Rewriting the solution with this condition in our notation and using the abbreviation $D=D(\omega)$, we have

$$N(r,t)=\frac{2}{Rr}\sum_{n=1}^{\infty}\exp\left\{-\frac{\pi^2n^2Dt}{R^2}\right\}$$

$$\times\sin\frac{n\pi r}{R}\int_0^R dr'r'f(r')\sin\frac{n\pi r'}{R}. \tag{6}$$

Here $f(r')$ is an initial condition, i.e., the distribution of particles at time $t=0$. In order to obtain the Green's function of interest to us from this, we need to reduce the size of the region r' where $f(r')$ is nonzero to zero, while the value of $f(r')$ in this region goes to infinity in such a way that the normalization condition for the total number of particles is satisfied:

$$4\pi\int_0^R dr'(r')^2f(r')=1. \tag{7}$$

Then from (6) we obtain

$$G(r,t)=\frac{1}{2R^2r}\sum_{n=1}^{\infty}n\exp\left\{-\frac{\pi^2n^2Dt}{R^2}\right\}\sin\frac{n\pi r}{R}. \tag{8}$$

The derivative $\partial G(r,t)/\partial r$ multiplied by D gives the local phonon flux at the point r at time t. Setting $r=R=1$ and multiplying the flux by the area of the sphere 4π we obtain the total phonon flux at frequency ω through a unit sphere at time t:

$$j(t)=2\pi^2D\sum_{n=1}^{\infty}(-1)^nn^2\exp(-\pi^2n^2Dt). \tag{9}$$

The value of the flux (9) computed for a number of values of the time t is shown in Fig. 2 by the large black dots against the background of smaller dots, which are the results of the simulation. It is clear that the agreement between the analytic values and the results of computer modeling in the range $t\gg\tau_i(\omega)$ is very good. This indicates that our program for simulating the kinetics of nonequilibrium phonons is operating correctly.

4. INCLUSION OF INELASTIC PROCESSES

The inclusion of decay processes considerably changes the phonon kinetics. Figure 3 shows computed time-of-flight spectra for various decay times τ when the initial phonons

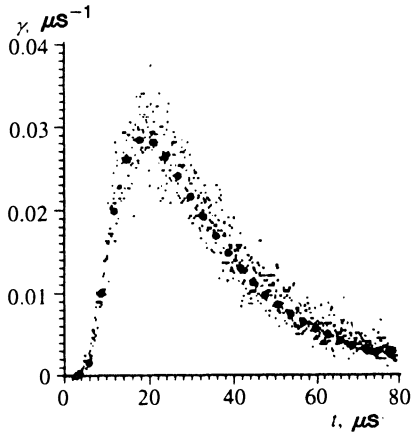

FIG. 2. Magnitude of the diffusion flux of nonequilibrium LA and TA phonons with frequency $\nu_0=1.0$ THz computed analytically using Eq. (9) for a series of values of the time t (large black dots), plotted against a background consisting of the results of numerical simulation of the phonon diffusion at the same frequency (small black dots).

start off as *LA* and *TA* with frequency 0.8 THz. As we already pointed out in Sec. 2, the value of the standard decay time τ_0 we used is one of the two values computed by Tamura[6] for two different experimental sets of parameters of the GaAs crystal: $\tau_0(\nu)=0.74\cdot10^{54}\nu^{-5}$ s. Because we cannot assume that this parameter has been accurately determined, and also because it may depend on the direction of the phonon quasimomentum vector, we carried out calculations for a number of different values of τ, expressed as multiples of τ_0.

A characteristic feature of the kinetics for initially *LA* phonons is the presence of clearly evident ballistic fluxes of both *LA* and *TA* phonons (Fig. 3a). The values of these fluxes increase as the decay time decreases: reducing τ by a factor of 16 leads to an increase in the ballistic flux of *TA* phonons by roughly a factor of 9. For decay times $\tau=\tau_0, 2\tau_0, 4\tau_0$ we observe broad but clearly discernible diffuse peaks; the positions of the maxima of these peaks approach that of the ballistic peak as we go from $4\tau_0$ to τ_0.

It is interesting to trace how the shape of the spectrum changes as the decay times take on the values $\tau=\tau_0/2$ and $\tau_0/4$. For these decay times there is no sign of a diffusive peak, and we clearly see a transition to the quasiballistic propagation regime for the phonons of the kind qualitatively discussed by Kazakovtsev and Levinson.[7]

Figure 3b shows the time-of-flight spectrum for starting phonons that are initially *TA* at the same frequency $\nu_0=0.8$ THz. It is clear that these initial conditions do not lead to the formation of the sharp ballistic peaks that are characteristic of simulations of the kinetics with initially *LA* phonons. On the contrary, a typical feature in this case is the presence of a "ballistic wall," i.e., an abrupt leading edge that smoothly transforms with increasing τ into a flux with a quasiballistic peak. This feature of nonequilibrium phonon pulses generated by initially *TA* phonons was first demonstrated by Lax *et al.*[14] using the Monte Carlo method; hence, the special case investigated in Ref. 14 is included within the general scheme of our results. The height of the wall and position of the pulse maximum depend on the anharmonic time τ. For

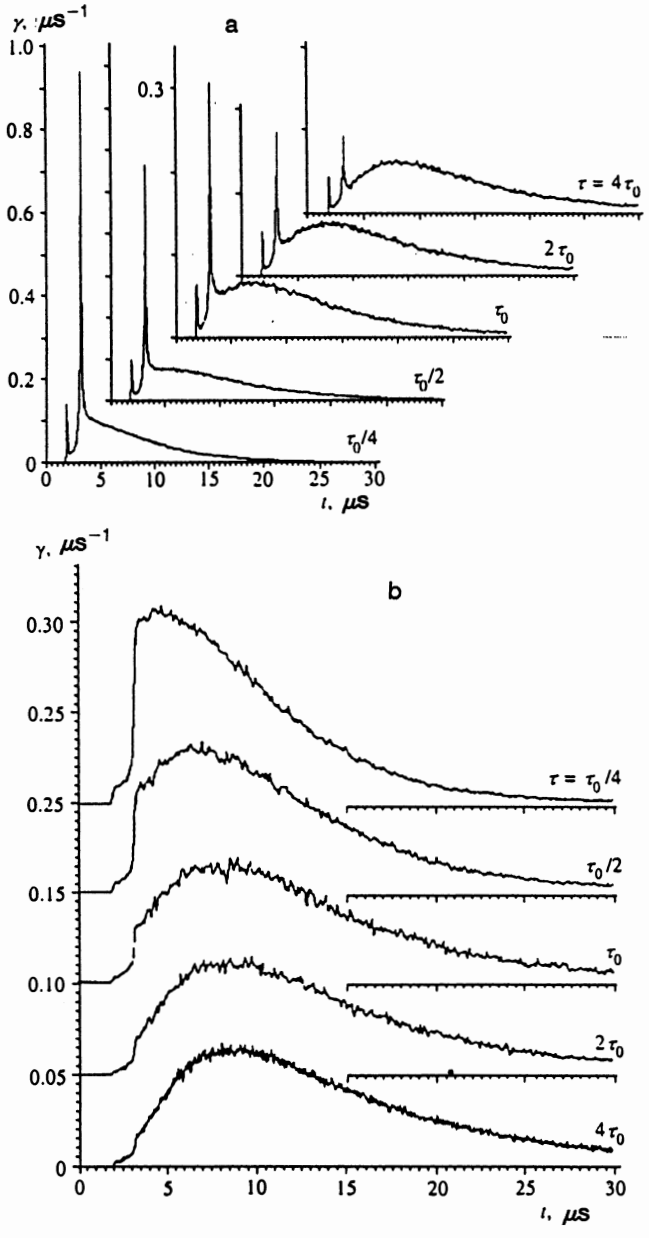

FIG. 3. Computed time-of-flight spectra of nonequilibrium phonons for various decay times τ for an initially starting LA (a) and TA (b) phonons with frequency ν_0=0.8 THz. In (a), the curves for $\tau=\tau_0$, $2\tau_0$, $4\tau_0$ are shown on a scale that is doubled along the ordinate; in (b) the curves are shifted along the ordinate for convenience of comparison.

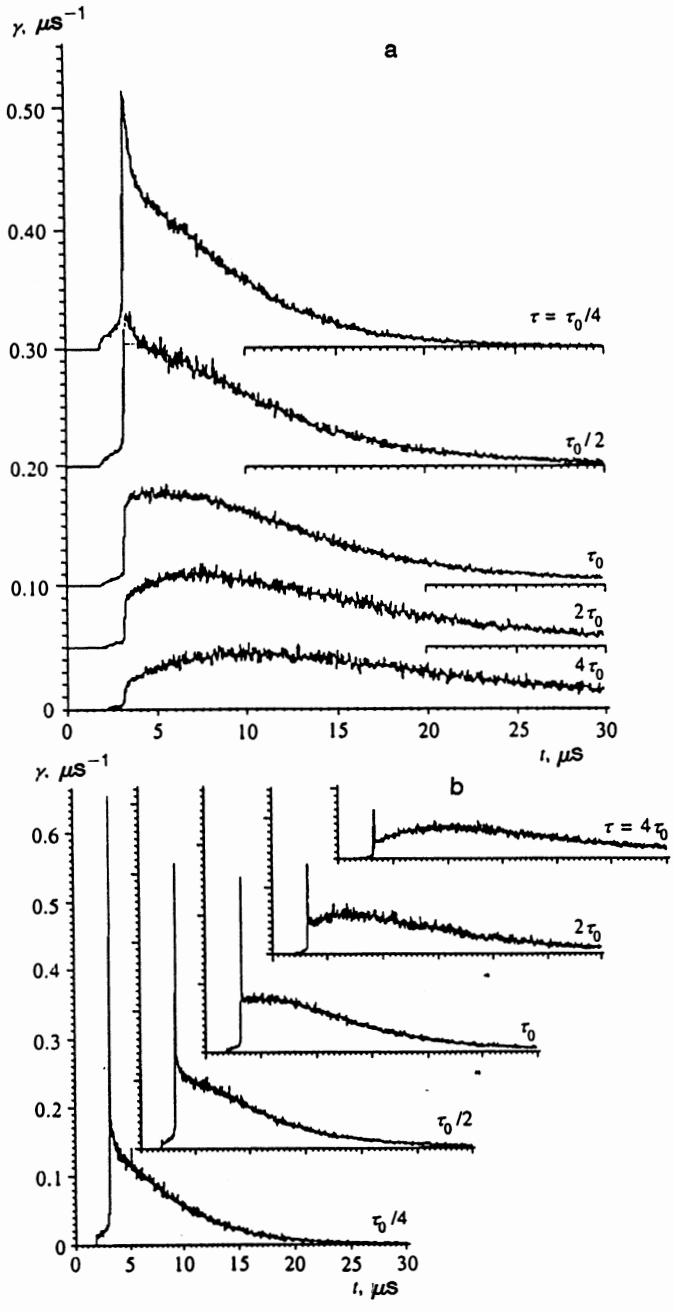

FIG. 4. Time-of-flight spectra of nonequilibrium phonons for initially TA (a) and LA (b) phonons with frequency ν_0=1.5 THz.

large decay times $\tau=2\tau_0$, $4\tau_0$ the position of t_{max} is close to that of the purely diffusive case. For the shorter decay times $\tau=\tau_0$, $\tau_0/2$, $\tau_0/4$ a characteristic transition is observed to a quasidiffusive propagation regime, with the position of the flux maximum a function of τ. However, for initially *TA* phonons with ν_0=0.8 THz, reducing the decay time even to $\tau_0/4$ does not drive the kinetics toward any clearcut quasiballistic regime.

Simulation results for phonon fluxes with the initial frequency 1.5 THz are shown in Fig. 4. First of all, we should note that for phonons with this frequency the maximum diffusive flux determined from Eq. (9) should be observed at times on the order of 100 μs. It was too expensive in computer time to simulate the diffusive regime of phonon propagation at this frequency, and we did not do it.

As is clear from Fig. 4a, initially *TA* phonons with ν_0=1.5 THz give rise to fluxes that are quite different from those with ν_0=0.8 THz shown in Fig. 3b. The distinctive feature is the transition of the time-of-flight spectra to quasiballistic behavior at decay times $\tau=\tau_0/2$ and $\tau_0/4$, as is clear from Fig. 4a. In addition, a comparison of the data of Fig. 3b and Fig. 4a shows that the ballistic component of the *TA* phonon flux is considerably larger for phonons with the initial frequency ν_0=1.5 THz than it is for phonons with ν_0=0.8 THz. Thus, e. g., for the standard decay time τ_0, the probability of ballistic flux comes to $\approx 3\cdot 10^{-3}$ for ν_0=0.8

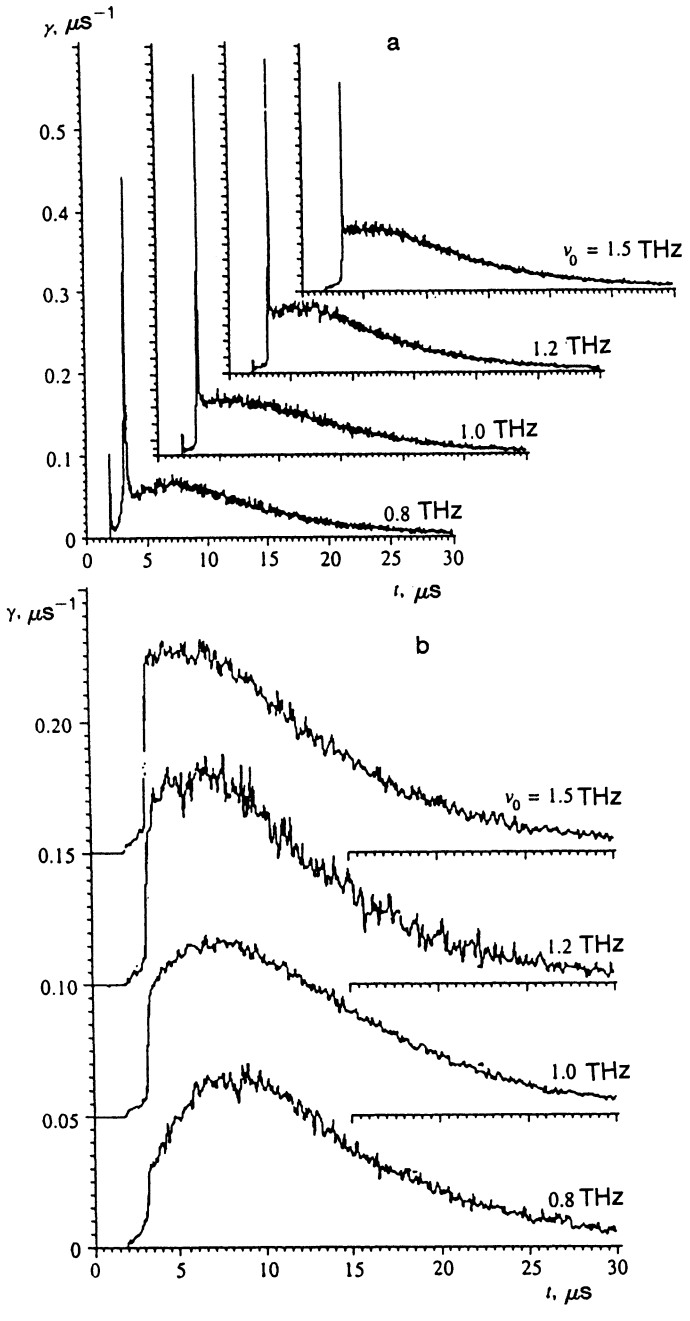

FIG. 5. Frequency dependence of the time-of-flight spectrum of nonequilibrium phonons for initially LA (a) and TA (b) phonons, using the standard decay time $\tau=\tau_0$.

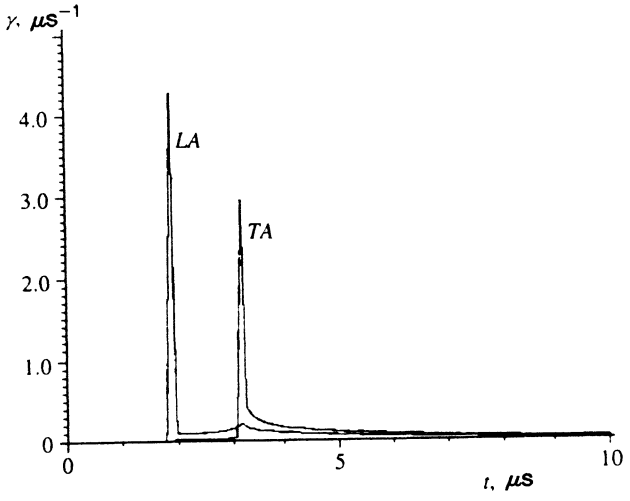

FIG. 6. Results of simulation of time-of-flight spectra of initially LA and TA phonons at frequency $\nu_0=0.5$ THz for the standard decay time $\tau=\tau_0$.

THz, whereas for $\nu_0=1.5$ THz this value of the probability is $\approx 8\cdot 10^{-3}$.

The plots shown in Figs. 4a and 4b exhibit some common features, notably a "ballistic wall" for the *TA* phonon flux and a weak "precursor" ballistic flux of *LA* phonons. This latter feature is almost absent for $\tau=4\tau_0$ but is easy to see for $\tau=\tau_0/4$. Quasidiffusion peaks are clearly evident for the decay times $\tau=\tau_0$, $2\tau_0$, $4\tau_0$; the position $t_{\max}$ of these peaks is a much stronger function of τ than it is for the case of initially *TA* phonons with $\nu_0=0.8$ THz.

The results of simulating fluxes generated by initially *LA* phonons with $\nu_0=1.5$ THz are shown in Fig. 4b. For phonons at these frequencies, the presence of a broad quasidiffusion peak whose position $t_{\max}$ depends on τ is also characteristic. In the figure it is evident how the transition occurs from the quasidiffusive form of the time-of-flight spectrum to one that is quasiballistic as the decay time decreases from $4\tau_0$ to $\tau_0/4$. Obvious ballistic fluxes of *TA* phonons are typical of initially *LA* phonons with both $\nu_0=0.8$ THz and $\nu_0=1.5$ THz. However, in contrast to the case $\nu_0=0.8$ THz, for $\nu_0=1.5$ THz there is essentially no ballistic *LA* peak.

As we have already noted, in a real experiment the initial acoustic phonons are created over a wide range of frequencies with a maximum at a characteristic frequency on the order of the Debye frequency. At this time, more detailed information about the initial spectral distribution of phonons is not available. Therefore, we present the individual time-of-flight spectra that correspond to sets of initial frequencies for *LA* and *TA* phonons and the standard decay time τ_0, keeping in mind that both these spectra enter into the real pulse shape with certain as yet unknown weights.

Figure 5 shows the results of simulating the phonon kinetics for various initial frequencies and the standard decay time $\tau=\tau_0$. It is clear that the decay of high-frequency *LA* phonons leads to a complex structure in the time-of-flight spectra. The latter are characterized by the presence of sharp ballistic *LA* phonon peaks associated with the decay of the original phonons at frequencies 0.8 and 1.0 THz, and also a sharp peak made up of ballistic *TA* phonons generated at all initial frequencies from 0.8–1.5 THz. These ballistic peaks are observed against a broad quasidiffusive background peak, whose position $t_{\max}$ shifts towards the ballistic *TA* peak with increasing frequency of the original *LA* phonon.

The quasidiffusive regime of phonon propagation is most evident in simulations of the propagation and relaxation of initially *TA* phonons. In this case ballistic peaks of *LA* and *TA* phonons do not form; however, the ballistic nature of the *TA* phonons is clearly identified by the presence of a

"wall." In this case, as follows from Fig. 5b, the amplitude of the latter increases as the original frequency ν_0 increases; however, this flux does not appear as an individual ballistic peak. Rather, the "ballistic wall" of *TA* phonon flux merges continuously into the wide quasidiffusion peak. The position of the quasidiffusion peak was observed to depend on the frequency of the original phonon. Thus, as the initial frequency varies from 0.8 to 1.5 THz, the position t_{max} shifts from $8\cdot10^{-6}$ s to $4\cdot10^{-6}$ s, i.e., it approaches that of the ballistic phonon flux, whose time-of-flight is $3.3\cdot10^{-6}$ s for phonons of the *TA* mode. This dependence of t_{max} on the frequency of the initial phonons is typical both of initially *LA* and initially *TA* phonons.

As the phonon frequency decreases, the probability of ballistic drift increases rapidly; this is reflected in the simulation results for phonons with ν_0=0.5 THz, as shown in Fig. 6.

5. ANALYSIS OF RESULTS AND COMPARISON WITH EXPERIMENT

Let us trace how the time-of-flight spectra obtained above reflect the experimentally observed features of the kinetics of high-frequency phonons in GaAs, in particular those already mentioned in Sec. 1. In our comparison we must take into account that the results of the simulation are semiquantitative in character, since we have not included anisotropic processes in our model of the phonon kinetics, which must depend on the specific crystal under study. Thus, for example, we have not taken into account that in certain crystallographic directions it is possible for phonons of the transverse branches to decay with the participation of a slow transverse *STA* mode of vibration as one of the final states. As was shown by Tamura *et al.*[18] and Berke *et al.*,[19] the probability of such a decay can be of the same order of magnitude as that of a decay into an *LA* phonon. It is also possible for the decay time τ to depend on the crystallographic direction. A dependence of this kind was calculated, e.g., by Tamura *et al.*[20] for crystals of germanium. Finally, focusing must necessarily influence the distribution of the ballistic phonon flux; we have also neglected this effect in formulating our model.

Nevertheless, the results of the simulation not only correspond qualitatively to the experimentally observed time-of-flight spectra in GaAs, but also exhibit the same features and details as the experimental curves. First of all, note that when the surface of GaAs is photoexcited, in almost every experiment we observe ballistic phonon peaks for all modes of vibration. Since the frequencies of the initially photoexcited acoustic phonons are $\approx$1.0–1.5 THz, these ballistic peaks can appear only as a result of processes whereby *LA* phonons present in the original spectrum decay spontaneously into two phonons with appreciably different frequencies. This follows directly from the results of Sec. 4 of this paper, as well as from a comparison with the simulation results of Refs. 12–14.

Furthermore, the simulation results clearly reveal the presence of a broad quasidiffusion peak whose maximum is located close to the frequency of the undecayed transverse mode of oscillation. An analogous phonon flux was observed by Danilchenko *et al.*[2] near the ⟨110⟩ direction in GaAs, and was referred to there the "*X*-peak." Starting with the solution to the time-dependent kinetic equations obtained in Ref. 2 for the phonon occupation numbers, it follows that the appearance of the "*X*-peak" is connected with spontaneous decay of high-frequency phonons. The results of the analysis given here imply that the time t_{max} at which the "*X*-peak" is a maximum should be less than the time for the appearance of a purely diffusive peak, and should depend on the frequency of the initial high-frequency phonon. Qualitatively, this dependence leads to a decrease in t_{max} with increasing frequency of the initial phonon. It follows from the results of this paper (Fig. 5b) that the position t_{max} of the quasidiffusion peak actually shifts toward small values with increasing frequency of the initial phonon, both for *LA* and *TA* modes. Thus, we have further evidence that the "*X*-peak" observed in GaAs is actually associated with the quasidiffusive regime of phonon propagation.

However, the authors of Ref. 2 did not observe quasidiffusive fluxes along the direction ⟨100⟩ in the same sample. The results of the simulation allow us to understand this fact qualitatively, if we assume that along this direction the decay time τ is 2 to 4 times smaller than the standard τ_0 obtained in the quasi-isotropic approximation. It follows from the time-of-flight spectra shown in Sec. 4 that reducing the decay time by a factor of 2 to 4 can change the phonon kinetics from quasidiffusive to quasiballistic. It is likely that this does happen in GaAs as we go from the direction ⟨110⟩ to the direction ⟨100⟩. A number of theoretical papers[19–21] have argued that the decay time should depend on the crystallographic direction.

This work was partially financed by grant NU5P000 of the International Science Foundation (the G. Soros fund).

[1] R. G. Ulbrich, in *Nonlinear Phonon Dynamics*, W. E. Beron ed., Plenum Press, New York (1985), p. 3.
[2] B. A. Danilchenko, V. N. Poroshin, M. I. Slutskiĭ, and M. Ashe, Phys. Status Solidi (b) **136**, 63 (1986).
[3] R. Orbach and L. A. Vredevoe, Physics **1**, 91 (1964).
[4] B. K. Rhee and W. E. Bron, Phys. Rev. B **34**, 7107 (1986).
[5] D. V. Kazakovtsev, A. A. Maksimov, D. A. Pronin, and I. I. Tartakovskiĭ, JETP Lett. **49**, 61 (1989).
[6] S. Tamura, Phys. Rev. B **31**, 2574 (1985).
[7] D. V. Kazakovtsev and I. B. Levinson, JETP Lett. **27**, 181 (1978).
[8] D. V. Kazakovtsev and I. B. Levinson, Phys. Status Solidi (b) **96**, 117 (1979).
[9] R. G. Ulbrich, V. Narayanamurti, and M. A. Chin, J. Phys. Soc. Jpn. **49**, Suppl. A 707 (1980).
[10] R. G. Ulbrich, V. Narayanamurti, and M. A. Chin, Phys. Rev. Lett. **45**, 1432 (1980).
[11] *Acoustic Crystals* [in Russian], M. P. Shaskol'skiĭ (ed.), Nauka, Moscow (1982), p. 167.
[12] M. Lax, V. Narayanamurti, and R. G. Ulbrich, in *Proc. 4th Intl. Conf. on Phonon Scattering in Condensed Matter*, Stuttgart, 1983, W. Eisenmenger, K. Lassman, and S. Dottinger (eds.), Springer-Verlag, Berlin (1984), p. 103.
[13] L. P. Wolfe and G. A. Northrop, in *Proc. 4th Intl. Conf. on Phonon Scattering in Condensed Matter*, Stuttgart, 1983, W. Eisenmenger, K. Lassman, and S. Dottinger (eds.), Springer-Verlag, Berlin (1984), p. 100.
[14] M. Lax, V. Narayanamurti, R. C. Fulton, and N. Holwarth, in *Proc. 5th Intl. Conf. on Phonon Scattering in Condensed Matter*, Urbana, 1986, A. C. Anderson and J. P. Wolfe (eds.), Springer-Verlag, Berlin (1986), p. 335.
[15] H. J. Maris, Phys. Rev. B **41**, 9736 (1990).
[16] D. V. Kazakovtsev, A. A. Maksimov, D. A. Pronin, and I. I. Tartakovskiĭ,

Zh. Eksp. Teor. Fiz. **98**, 1465 (1990) [Sov. Phys. JETP **71**, 819 (1990)].
[17] G. Carlslow and D. Eger, *Thermal Conductivity of Solids* [in Russian], Nauka, Moscow (1964), p. 230.
[18] S. Tamura and H. J. Maris, Phys. Rev. B **31**, 2595 (1985).
[19] A. Berke, A. P. Mayer, and R. K. Wehner, Solid State Commun. **54**, 395 (1985).
[20] S. Tamura and K. Okubo, *Acoustic Crystals* [in Russian], M. P. Shaskol'skiĭ (ed.), Nauka, Moscow (1982), p. 109.
[21] M. T. Labrot, A. P. Mayer, R. K. Wehner, and P. E. Obermayer, J. Phys. Cond. Matter **1**, 8809 (1989).

Translated by Frank J. Crowne